WILEY InterScience® DISCOVER SOMETHING GREAT

PROTEINS STRUCTURE ■ FUNCTION ■ BIOINFORMATICS

STRUCTURE NOTE

The crystal structure of the catalytic domain of the chick retinal neurite inhibitor—receptor protein tyrosine phosphatase CRYP-2/cPTPRO

T.S. Girish and B. Gopal*

Molecular Biophysics Unit, Indian Institute of Science, Bangalore 560 012, India

INTRODUCTION

Chick retinal tyrosine phosphatase-2 (CRYP-2) is a type-III receptor protein tyrosine phosphatase (RPTP) that is selectively expressed in neurons and has been implicated in axon growth and guidance.[1] The extracellular domain of CRYP-2 has eight fibronectin type-III repeats and has been demonstrated to inhibit neurite outgrowth, mediate growth cone collapse as well as serve as a repulsive guidance cue for retinal axons.[2] Two major classes of RPTPs, type II and type III play a major role in the axon guidance process.[1,3] The role of these RPTPs as well as the mechanism(s) by which activity is regulated has been extensively examined for some proteins belonging to the type II family that includes LAR (leukocyte common antigen related), PTP-δ, and PTP-σ in both *Drosophila* as well as chick model systems of axonal growth and development. However, apart from genetic data that suggests that competition between the type II and type III family of proteins regulates motor axon growth, relatively little is known of proteins that belong to the type III family. Inferences on the role and regulatory mechanisms of type III RPTPs based on substrate preferences are inconclusive due to both, the diversity of interacting proteins and the range of cellular processes involved. The type III RPTP density enhanced phosphatase-1 (DEP-1) implicated in tumorogenesis, for example, has been shown to interact with the PDGF receptor, the hepatocyte growth factor receptor, and p120(ctn).[4] The catalytic domain of CRYP-2 shares a close sequence similarity to DEP-1 (65%) and interacts with the neuronal pentraxin with chromo-domain.[1] Thus while diversity in interacting partners for type-III RPTPs suggests a range of downstream signaling pathways, the mechanism by which the activity of the catalytic domain is regulated is yet unknown. The catalytic domain of CRYP-2 is almost identical (ca. 98% sequence identity) to human PTPRO, a protein implicated as a growth regulatory factor in hepatocellular carcinomas.[5] Homologous type III RPTPs, PTP10D, and PTP52F, play a major role in axon guidance in *Drosophila*.[3] An understanding of the substrate specificity as well as regulatory mechanism of this protein could thus serve to reconcile the various roles played by this RPTP and its homologues in different cellular and developmental contexts.

Here we present the crystal structure of CRYP-2 that shows two molecules of CRYP-2 in the asymmetric unit. The substantial buried surface area of this crystallographic oligomer suggested a homo-dimer of the catalytic domain. Subsequent solution studies suggested that this protein is a monomer in solution based on the elution profile of CRYP-2 in a size exclusion chromatography experiment. The monomeric nature of the catalytic domain of CRYP-2 thus distinguishes members of the PTPRO family from the well characterized dimeric

Grant sponsors: Department of Biotechnology and the Department of Science and Technology, Government of India.
*Correspondence to: B. Gopal; Molecular Biophysics Unit, Indian Institute of Science, Bangalore 560 012, India. E-mail: bgopal@mbu.iisc.ernet.in
Received 21 November 2006; Accepted 8 January 2007
Published online 1 June 2007 in Wiley InterScience (www.interscience.wiley.com).
DOI: 10.1002/prot.21424

RPTP-α family of PTP's, where a helix-turn-helix segment of one monomer blocks the active site of the other. Both monomers of CRYP-2 in the crystal have a nitrate ion bound at the active site. An advantage provided by the crystallographic dimer of CRYP-2 was that it allowed us to visualize this protein with its active site lid (WPD loop) in both the open and closed conformations. A structural comparison of the catalytic domain of CRYP-2 with other PTP's also reveals variations in residues that line the so-called "secondary site."[6] This adaptable region has previously been demonstrated to be crucial for the design of selective, noncompetitive PTP inhibitors that function by stabilizing a conformation of the WPD-loop associated with the inactive state.

Table I
Data Collection and Refinement Statistics

Data collection	
Space group	$P3_12\ 1$
Cell dimensions	$a = b = 68.3$ Å, $c = 245$ Å
Resolution (Å)	42.56–2.59 (2.73–2.59)[a]
R_{merge} (%)	11.61 (34.5)
$I/\sigma I$	10.0 (3.3)
Completeness (%)	97.3 (81.6)
Multiplicity	3.6 (3.4)
Refinement	
Resolution (Å)	20.0–2.6
No. of reflections	21,113 (2,531)
R_{work}/R_{free}	23.64/28.35
No of atoms	
Protein	4,711
Ligand/ion	2
Water	182
R.m.s deviations	
Bond lengths (Å)	0.014
Bond angles (°)	1.8

[a]Outer Resolution shell.

MATERIALS AND METHODS

Cloning, expression, and purification of wild type CRYP-2 and its point variants

On the basis of an expression analysis with different protein sizes, the gene encoding residues 956-1267 in either the pET-15b (that yields a recombinant protein with a poly-histidine tag at the N-terminus) or pET-22b (recombinant protein with a poly-histidine tag at the C-terminus) vectors provided the best yields of recombinant protein. Thus recombinant CRYP-2 encoding residues 956-1267 with a poly-histidine tag at the C-terminus was used in the structural studies reported in this manuscript. The details of the cloning, expression, and purification of CRYP-2 has been reported earlier.[7] Briefly, *E. coli* BL21(DE3)PLysS cells containing the plasmid of interest were grown to an optical density of 0.5 at 600 nm, whereupon the cells were induced with 0.4 m*M* IPTG (final concentration). Following this, the temperature for growth was lowered to 290 K and cells were grown for a further 6 h before they were spun down and stored at 193 K until use. The cells were resuspended in lysis buffer (50 m*M* sodium phosphate buffer, 250 m*M* NaCl, pH 7.5). After sonication for 4 min on ice, the cell debris was separated from the crude cell lysate by centrifugation for 30 min at 10,000 rpm in a Sorvall centrifuge. After equilibration with cobalt-containing Talon resin (Clontech) and a washing step with buffer B (50 m*M* sodium phosphate, 250 m*M* NaCl, 5 m*M* imidazole, pH 7.5), the recombinant protein was eluted from the column by a gradient of imidazole concentration ranging from 5 m*M* to 200 m*M* in 50 m*M* sodium phosphate and 250 m*M* NaCl, pH 7.5. The partially purified protein was further subjected to size-exclusion chromatography on a Sephacryl Hiprep 16/60 S-200 HR column (Amersham Biosciences) in a buffer containing 50 m*M* Tris-HCl, 250 m*M* NaCl, and 3 m*M* EDTA at pH 7.5.

Determination of the crystal structure

The crystallization and data statistics for CRYP-2 have been reported earlier.[7] A single crystal of CRYP-2 was flash frozen using 15% PEG 400 as the cryo-protectant. It was essential that the cryo-protectant buffer contained 1–5 m*M* Dithiotrietol (DTT) to reduce the diffraction spot mosaicity. The diffraction data were collected at 100 K on a MAR imaging-plate system mounted on a Rigaku RU-200 rotating-anode X-ray generator. The data were processed using MOSFLM[8] and were scaled using SCALA.[9] The initial phases were obtained by molecular replacement with the program PHASER[10] using PTP-μ (1 RPM) as the search model.[11] The molecular replacement solution had a *Z*-score of 15.7 and log likelihood gain of 618.02. After 50 cycles of rigid body refinement

Figure 1
*(**a**) Sequence alignment of PTP D1 domains of CRYP-2, RPTP-α and RPTP-μ, and PTP1B. The secondary structure elements corresponding to CRYP-2 are shown. A grey background has been used to highlight residues involved in oligomerization. These are poorly conserved. (**b**) The quaternary arrangement of CRYP-2 showing the location of the two active sites. The active site of CRYP-2 (highlighted by the red circle) is not occluded by oligomerization. The active site cysteine, aspartate, proline, tryptophan, and the bound nitrate ion are depicted in ball and stick representation. (**c**) Both open and closed conformations of the active site lid are seen in the crystal structure. In this superposition, the red ribbon representation is for CRYP-2 while the superposed PTP1B conformation is seen in grey. (**d** and **e**) The active site of CRYP-2 contains a nitrate ion in both the closed and open conformations. Panels d (closed conformation) and e (open conformation) show the (2Fo–Fc) electron density map calculated at 1.2 σ for the residues that surround the active site as well as the bound nitrate ion.*

DOI 10.1002/prot

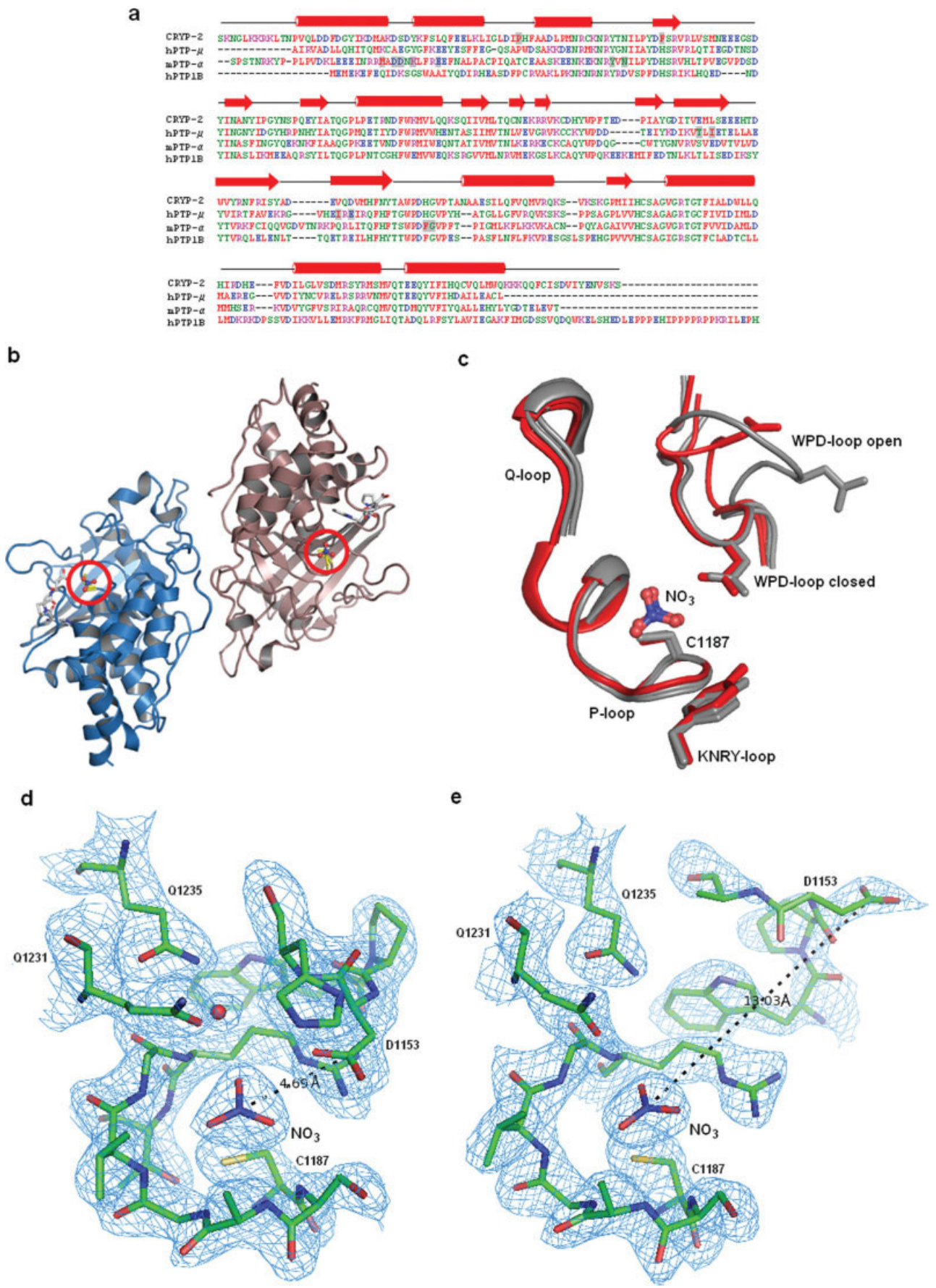
a
CRYP-2
hPTP-μ
mPTP-α
hPTP1B
b
c
Q-loop
WPD-loop open
WPD-loop closed
NO3
C1187
P-loop
KNRY-loop
d
Q1235
Q1231
D1153
4.69 Å
NO3
C1187
e
Q1235
D1153
Q1231
13.03Å
NO3
C1187

Figure 1

Table II
Comparison of Kinetic-Parameters of CRYP-2 and its Point Variants

Protein	K_m (m*M*)	V_{max} (μmol mnt^{-1} mg^{-1})	K_{cat} (s^{-1})	K_{cat}/K_m (M^{-1} s^{-1})
CRYP2-WT	1.33 ± 0.15	160.8 ± 5.0	100.65 ± 3.15	7.05 ± 0.77 × 10^4
C1090S MUTANT	2.07 ± 0.11	29.5 ± 1.25	18.55 ± 0.78	7.57 ± 0.21 × 10^3
C1098S MUTANT	2.85 ± 0.07	73.96 ± 3.67	46.50 ± 2.32	15.92 ± 1.0 × 10^3
C1187S MUTANT	2.56 ± 0.13	0.40 ± 0.01	207.05 ± 31.85 × 10^{-3}	86.9 ± 8.2

using CNS,[12] the electron density map was calculated for the model. Model building was performed using COOT.[13] After each step of model building, positional and B-factor refinement were carried out. The data collection and refinement statistics are presented in the Table I.

Determination of the kinetic constants

Activity measurements were performed using *para*-nitrophenyl phosphate (*p*NPP) as substrate. The assay buffer had 25 m*M* HEPES, 50 m*M* NaCl, 5 m*M* DTT, and 2.5 m*M* EDTA at pH 7.0 ± 0.2. The final reaction volume (200 μL) contained 90 μL of BSA (0.01%) solution, 80 μL of assay buffer, and 20 μL of *p*NPP substrate (from a fresh stock of 50 m*M* concentration). The reaction was started by adding 10 μL of purified enzyme followed by incubation for 10 min at 37°C. The reaction was stopped by adding 100 μL of 2.0*M* Na_2CO_3 solution. After this step, the volume was adjusted to 1000 μL by the addition of 700 μL of water and the absorbance was monitored at 405 nm. The enzyme activity was calculated by monitoring the product formed using the extinction coefficient of 1.78 × 10^4 M^{-1} cm^{-1} for *para*-nitrophenol. One unit of activity is equivalent to 1.0 nanomol of *p*NPP hydrolyzed per minute. The data were analyzed using non-linear regression hyperbolic fitting to a classical Mechalis-Menten model using the Sigma-Plot software (Systat Software).

RESULTS AND DISCUSSION

Structure determination and enzymatic characterization of the catalytic domain of CRYP-2

There are two molecules of CRYP-2 in the asymmetric unit of the crystal [Fig. 1(b)]. This protein, however, is a monomer in solution as seen by its mobility in a size exclusion chromatographic experiment performed at a 2.0 mg mL^{-1} concentration. The overall structure of CRYP-2 resembles closely to that of the catalytic domain of RPTPμ[11] (sequence identity 42.0%; RMSD of Cα atoms 1.2 Å) with α-helices flanking twisted β-sheets. An interesting feature of the PTP family of proteins is that in spite of a highly conserved three-dimensional structure, certain conformational variations determine the regulation of function. In the case of RPTP-α, for example, the conserved catalytic cysteine residue can form an intermolecular disulfide bond. Dimerization of RPTP-α also involves a structural arrangement whereby a helix-turn-helix segment of one monomer blocks the active site of the other.[14] While the monomeric nature of CRYP-2 precludes the possibility of a regulatory mechanism involving oligomerization, potential modulation of activity by disulfide bond formation involving the active site cysteine was experimentally evaluated. A structural comparison of CRYP-2 with other PTPs reveals the presence of two cysteine residues in close proximity to the active site. Point variants of CRYP-2 were engineered to investigate the role, if any, of these residues in regulating the activity of this protein. Thiol estimation experiments using Ellman's reagent show that two out of six cysteines in the catalytic domain of CRYP-2 are buried in native conditions. However, thiol estimation in denaturing conditions in the absence of any reducing agent unambiguously shows that none of the cysteines in CRYP-2 are involved in disulfide bonds. Indeed, point variations of the structurally proximal cysteine residues show a slight reduction in activity as compared to the wild type protein. The results of the activity measurements of CRYP-2 and the cysteine point variants are summarized in Table II.

WPD loop conformation

A well ordered trigonal planar-shaped electron density was observed near the catalytic Cys-Sγ atom from the early stages of refinement. This was modeled and refined as a nitrate ion as the crystallization mother liquor contained 0.5*M* Ammonium nitrate. This electron density for the nitrate ion was seen at the active site of both the subunits. The main differences in the two monomers of CRYP-2 lie in the conformation of the active site lid, the so-called WPD loop. The WPD loop adopts an open conformation in one monomer and a closed conformation in the other (definitions of open and closed conformations have been adapted from PTP1B[15,16]). While continuous and well defined electron density was observed for the WPD loop residues in the closed conformation at the active site of subunit A, the electron density for the WPD loop of the B subunit is rather

DOI 10.1002/prot

poor. Nonetheless, key residues that are involved in substrate recognition could be clearly modeled into the electron density for both conformers [Figs. 1(d,e)]. The presence of a bound nitrate ion at the active site in either conformation of the WPD loop suggests that the rapid changes in the loop conformation are possible. The structure of the catalytically competent (closed) and inactive (open) WPD loop conformations of CRYP-2 provide a structural framework for the design of noncompetitive inhibitors specific to the PTPRO family. Efforts to identify noncompetitive inhibitors of PTP1B that are not phospho-tyrosine mimics and thus provide higher selectivity led to the identification of a so-called secondary site situated about 20 Å away from the active site.[6] The benzbromarone derivatives that were used in these studies function by stabilizing the inactive (open) conformer of the WPD loop. The predominantly hydrophobic pocket in PTP1B that facilitates the binding of these noncompetitive inhibitors is substantially different in CRYP2 because of the replacement of key residues Phe196 and Phe280 by glutamine and lysine, respectively. These residues are conserved in the human homologue of CRYP-2, hPTPRO, a protein implicated in hepatocellular carcinomas.[5] The modified secondary site of CRYP-2 could thus provide a structural basis for the design of selective, noncompetitive inhibitors for the PTPRO class of tyrosine phosphatases. The crystal structure has been deposited in the PDB (Code 2PI7).

ACKNOWLEDGMENT

BG is an International Senior Research Fellow of the Wellcome Trust, UK.

REFERENCES

1. Chen B, Bixby JL. A novel substrate of receptor tyrosine phosphatase PTPRO is required for nerve growth factor-induced process outgrowth. J Neurosci 2005;25:880–888.
2. Stephanek L, Sun QL, Wang J, Wang C Bixby JL. CRYP-2/cPTPRO is a neurite inhibitory repulsive guidance cue for retinal neurons in vitro. J Cell Biol 2001;154:867–878.
3. Johnson KG, Van Vactor. Receptor protein tyrosine phosphatases in nervous system development. Physiol Rev 2003;83:1–24.
4. Palka HL, Park M, Tonks NK. Hepatocyte growth factor receptor tyrosine kinase met is a substrate of the receptor protein-tyrosine phosphatase DEP-1. J Biol Chem 2003;278:5728–5735.
5. Motiwala T, Ghoshal K, Das A, Majumder S, Weichenhan D, Wu Y-Z, Holman K, James SJ, Jacob ST, Plass C. Suppression of the protein tyrosine phosphatase receptor type O gene (PTPRO) by methylation in hepatocellular carcinomas. Oncogene 2003;22:6319–6331.
6. Weismann C, Barr KJ, Kung J, Zhu J, Erlanson DA, Shen W, Fahr BJ, Zhong M, Taylor L, Randal M, McDowell RS, Hansen SK. Allosteric inhibition of protein tyrosine phosphatase 1B. Nat Struct Mol Biol 2004;11:730–737.
7. Girish TS, Gopal B. Crystallization and preliminary X-ray diffraction studies on the catalytic domain of the chick retinal neurite-inhibitory factor CRYP-2. Acta Cryst 2005;F61:381–383.
8. Leslie AGW. Recent changes to the MOSFLM package for processing film and image plate data. Joint CCP4 + ESF-EAMCB Newsletter on Protein Crystallography 1992;26.
9. Collaborative Computational Project, Number 4. The CCP4 Suite: programs for Protein Crystallography. Acta Cryst 1994;D50:760–763.
10. Storoni LC, McCoy AJ, Read RJ. Likelihood-enhanced fast rotation functions. Acta Cryst 2004;D60:432–438.
11. Hoffmann KMV, Tonks NK, Barford D. The crystal structure of domain 1 of receptor protein tyrosine phosphatase μ. J Biol Chem 1997;272:27505–27508.
12. Brunger AT, Adams PD, Clore GM, DeLano WL, Gros P, Grosse-Kustleve RW, Jiang JS, Kuszewski J, Nilges M, Pannu NS, Read RJ, Rice LM, Simonson T, Warren GL. Crystallography and NMR system: a new software suite for macromolecular structure determination. Acta Cryst 1998;D54:905–921.
13. Emsley P, Cowtan K. Coot: model-building tools for molecular graphics. Acta Cryst 2004;D60:2126–2132.
14. Bilwes AM, Den HJ, Hunter T, Noel JP. Structural basis for inhibition of receptor protein tyrosine phosphatase-α by dimerization. Nature 1996;382:555–559.
15. Barford D, Flint AJ, Tonks NK. Crystal structure of human protein tyrosine Phosphatase 1B Science 1994;263:1397–1404.
16. Jia Z, Barford D, Flint AJ, Tonks NK. Structural basis for phosphotyrosine peptide recognition by protein tyrosine phosphatase 1B. Science 1995;268:1754–1758.